J. Biomed. Eng. Res.
Vol. 25, No. 3, 189-194, 2004

부분 히스토그램 문턱치 알고리즘을 사용한 조영증강 CT영상의 자동 간 분할

서경식[1], 박승진[2], 박종안[3]

[1]Electrical & Computer Engineering, New Mexico State University, Las Cruces, USA.
[2]전남대학교병원 의공학과, [3]조선대학교 공과대학 정보통신공학과
(2004년 1월 15일 접수, 2004년 5월 22일 채택)

Automatic Liver Segmentation of a Contrast Enhanced CT Image Using a Partial Histogram Threshold Algorithm

Kyung-Sik Seo[1], Seung-Jin Park[2], Jong An Park[3]

[1]Electrical & Computer Engineering, New Mexico State University, Las Cruces, USA.
[2]Dept. of Biomedical Engineering, Chonnam Univ. Hospital, Gwangju, Korea.
[3]Electronics Information & Communications Engineering, Chosun University
(Received January 15, 2004. Accepted May 22, 2004)

요 약 : 조영 증강된 CT 영상의 화소값은 조영제에 의해 이산적으로 변한다. 또한 간의 중간부분에서는 간과 유사한 농도값을 갖는 췌장 때문에 간의 분할이 어렵다. 본 논문에서는 조영증강된 CT영상의 화소값의 이산적인 변화와 간과 겹치는 췌장을 제거하기 위하여 부분 히스토그램 문턱치 알고리즘을 사용한 간 분할법을 제안한다. 히스토그램 변환 후 간 구조의 농도 값의 범위를 찾기 위한 적응 다봉성 분할과 췌장 제거를 위한 부분 히스토그램 문턱치 알고리즘을 수행한다. 다음으로, 간 이외의 불필요한 대상을 제거하고 경계를 매끈하게 하기 위해 모폴러지 필터링을 수행한다. 제안된 방법을 평가하기 위해 8명의 환자로부터 획득된 CT영상중 중간부분에서 4개씩 총 32단면을 선택하였다. 부분 히스토그램 문턱치 알고리즘을 사용한 자동 분할법 II와 수동 분할법의 정규화된 평균 면적의 평균은 0.1671과 0.1711이었으며, 이 두 방법은 아주 적은 차이를 보인다. 또, 자동 분할법 II 와 수동 분할법의 평균 면적 오차율은 6.8339 % 이다. 이 실험 결과로부터 제안된 자동 간분할 법은 의사에 의해 시행된 수동 분할법과 매우 유사한 수행능력을 갖는다.

Abstract : Pixel values of contrast enhanced computed tomography (CE-CT) images are randomly changed. Also, the middle liver part has a problem to segregate the liver structure because of similar gray-level values of a pancreas in the abdomen. In this paper, an automatic liver segmentation method using a partial histogram threshold (PHT) algorithm is proposed for overcoming randomness of CE-CT images and removing the pancreas. After histogram transformation, adaptive multi-modal threshold is used to find the range of gray-level values of the liver structure. Also, the PHT algorithm is performed for removing the pancreas. Then, morphological filtering is processed for removing of unnecessary objects and smoothing of the boundary. Four CE-CT slices of eight patients were selected to evaluate the proposed method. As the average of normalized average area of the automatic segmented method II (ASM II) using the PHT and manual segmented method (MSM) are 0.1671 and 0.1711, thesre two method shows very small differences. Also, the average area error rate between the ASM II and MSM is 6.8339 %. From the results of experiments, the proposed method has similar performance as the MSM by medical Doctor.
Key words : Computed Tomography, Contrast enhancement, Histogram Transform, Piecewise linear interpolation, Partial histogram threshold.

INTRODUCTION

Liver cancer is included in fifth main cancers such as lung, breast, colorectal and stomach in the world. It is more serious in eastern and southeastern Asia areas including western and central Africa [1]. The average incidence of liver cancer in this area is 20 per 100,000 and liver cancer is the third highest cause of death from cancer [1]. In Korea, the incidence of a liver cancer is quite high at 19% for male and 7% for female [2]. New cases of liver cancer in the Seoul area have an approximate rate per year as 34.1 for male and 11.5 for female per 100,000 people [2]. Prevention is by far the best way to reduce liver cancer as with other cancers. Besides prevention, the early detection and treatment of liver cancer is critical. If the liver is analyzed for early detection, treatment and curing may be easy and human life can be prolonged.

통신저자 : 박승진, (501-757) 광주광역시 동구 학 1동 8
전남대학교병원 의공학과
Tel. 062)220-6070, Fax. 062)226-4762,
E-mail. sjinpark@cnuh.chonnam.ac.kr

In order to segregate hepatic tumors, the first significant process is to extract the liver structure from other abdominal organs. Liver segmentation using CT images has been dynamically performed because CT is a very conventional and non-invasive technique. Sungkee Lee [3] extracted the liver using Co-occurrence matrix from CT as the automatic method. Bae et al [4] used priori information about liver morphology and image processing techniques such as gray-level thresholding, Gaussian smoothing, mathematical morphology techniques, and B-splines. Gao et al [5] developed automatic liver segmentation using a global histogram, morphologic operations, and the parametrically deformable contour model. Tsai [6] proposed an alternative segmentation method using an artificial neural network to classify each pixel into three categories. Also, Husain et al [7] used neural networks for feature based recognition of liver region.

Generally, in order to improve diagnosis efficiency of the liver, the CT image is obtained by contrast media. Pixel values of contrast enhanced CT (CE-CT) images acquired from the dose of contrast agent are randomly changed. Also, the middle liver part has a problem to segregate the liver structure because of similar gray-level values of a pancreas in the abdomen. In this paper, an automatic liver segmentation method using a partial histogram threshold (PHT) algorithm is proposed for overcoming pixel variation of CE-CT images and removing the pancreas which is contact with liver. In the following section, liver segmentation is performed regardless of randomness of CE-CT images. Also, we demonstrate experiments and their analysis results. Finally, the conclusion will be given in the last section.

LIVER SEGMENTATION

In this section, liver segmentation is presented. Histogram transform (HT) such as convolution and scaling is described to reduce histogram noise. The adaptive multi-modal thresholding (AMT) method is performed to find the range of gray-level values of the liver structure. Also, the partial histogram thresholding algorithm is proposed to remove the pancreas. Then, binary morphological (BM) filtering is processed for removing of small unnecessary objects and smoothing of the boundary. Liver segmentation is described as the block diagram of Fig. 1.

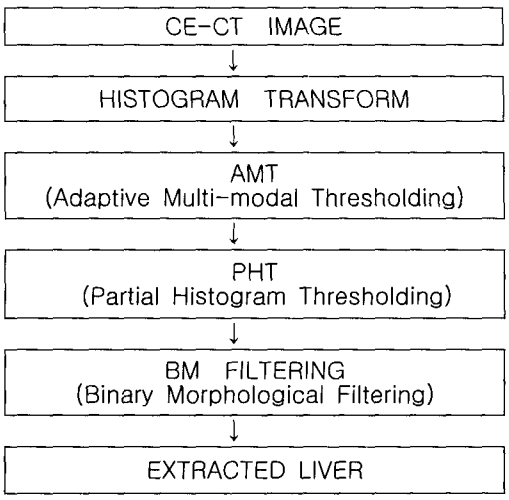

Fig. 1. The overall block diagram of the proposed liver segmentation algorithms.

1. Histogram Transform

In spite of the disadvantage of the pixel variation caused by the contrast enhancement, the CE-CT image gives an advantage of pixel enhancement. Pixel enhancement using a contrast medium comes from increasing the attenuation value of tissue difference between liver and other organs. Pixel variation provides a multi-modal histogram and creates easier segmentation of the histogram.

The histogram in pixel-based segmentation can be used simply to provide statistical information like mean, median, standard deviation, and energy. The histogram is a one-dimensional statistical transformation obtained by counting total pixel numbers for each gray level. Let $I: Z^2 \rightarrow Z$ be a gray-level CE-CT image and (m, n) be a pixel location. Then, $I(m, n) Z^2 \rightarrow Z \in Z$. Also, the histogram, $h(k): Z \rightarrow Z$, is defined as [8]

$$h(k) = \{(m, n) \mid I(m, n) = k\} \quad (1)$$

where k is a gray-level value.

The histogram has small noise to hinder multi-modal thresholding. To reduce small noise, histogram transform such as convolution and scaling is proposed. A convolution method as one dimensional low pass filtering is used to smooth the histogram, even though the histogram's horizontal axis is extended and a vertical axis is very increased [9]. Then, the extended horizontal axis is scaled to gray-level values by a factor β A convolved histogram, $h': Z \rightarrow Z$, is defined as

$$h' = h * g \quad (2)$$

where g is a one dimensional function. A scaled histogram, $h_s: Z \rightarrow Z$, is defined as

$$h_s = \frac{1}{\beta} h' \tag{3}$$

where β is a scaling factor.

2. Adaptive Multi-Modal (AMT) Thresholding

For solving given pixel variation of a CE-CT image, an AMT method is used. The AMT method is processed regardless of histogram variation derived from the contrast enhancement. First of all, after removing the background, bones and extremely enhanced organs such as vessels, we find a global peak in the multi-modal histogram. The left and right valleys are calculated using a piecewise linear interpolation (PLI) method. The PLI method [10] calculates the slope, $f_k: Z \rightarrow Z$, as the line segment from $(k, h_s, (k))$ to $(k+\gamma, h_s(k+\gamma))$ and its formula is given as

$$f_k = \frac{h_s(k+\gamma) - h_s(k)}{(k+\gamma) - k} \tag{4}$$

where γ is an integer.

Each valley may be founded at the turning point from a negative value to a positive value because each point represents the slope. Left and right valleys become one range of an object. Then, the extracted range is removed from h_s and this process is repeated until several ranges are found. The important range in this research is the range including gray-level values of the liver. The liver range is located experimentally in the right side of the histogram because of pixel enhancement of CE-CT images. Let $[k_1, k_2]$ be the extracted lower and upper thresholding integer values containing pixels of the gray-level liver region. Then each $I_{liver}: Z^2 \rightarrow Z^2$ is defined as

$$I_{liver} = \{(m, n) \mid k_1 \leq I(m, n) \leq k_2\} \tag{5}$$

Fig. 2 shows the example of the AMT method. Fig. 2(a) is a gray-level CT image obtained from a CE-CT image and Fig. 2(b) is a histogram, $h(k)$, with multi-modal distribution based on gray-level values. Transformed histogram using convolution and scaling is displayed in Fig. 2(c). Fig. 2(d) is gray-level images after the AMT method. Fig. 2(e) is the image after unnecessary small objects are removed.

3. Partial Histogram Thresholding (PHT) Algorithm

If the liver has similar point values with other organs, I_{liver} created from AMT may not be segregated successfully. As the histogram of I_{liver} is uni-modal shape, it is too hard to use various thresholding methods. In order to get away from difficult segmentation, a PHT algorithm which performs better liver segmentation is proposed. This algorithm transforms a given partial gray-level range to a broad range with keeping the order of gray-levels.

Let $h_{liver}(k_1, k_2): Z \rightarrow Z$ be the histogram of I_{liver} with the range, $[k_1, k_2]$. Let I_P be the PHT image. Then the PHT algorithm is proposed:

- Find k_{max} where k_{max} is the gray-level value when $h_{liver}(k)$ is the maximum value.
- Calculate partial histogram interval
  $k_\Delta = (k_{max} - k_\Delta)/\Delta$
  where Δ is the integer value greater than 0.

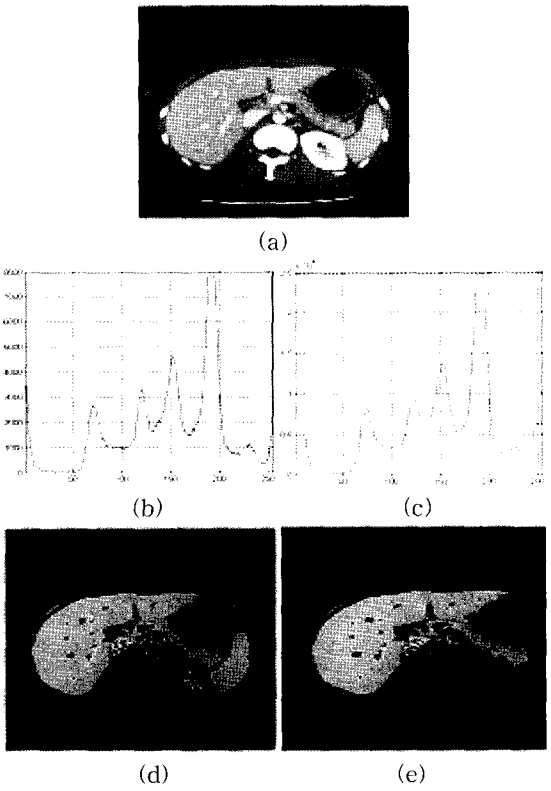

Fig. 2. AMT(AdaptiveMulti-modal Thresholding): (a) gray-level CE-CT image, (b) histogram, $h(k)$, (c) transformed histogram, h_s (d) I_{liver} after AMT, and (e) I_{liver} after small objects are removed.

- Find the partial threshold value $k_p = (k_{max} - k_\Delta)$.
- Create the PHT image I_P
  $I_P = \{(m, n) \mid k \leq I_{liver}(m, n) \leq k_p\}$.

After obtaining I_P by the PHT algorithm, I_{diff} is calculated from $I_{liver} - I_p$.

Fig. 3 (a) shows the histogram of I_{liver}. (b) is the

PHT image, I_P and (c) shows I_{diff} which represents image difference between I_{liver} and I_P.

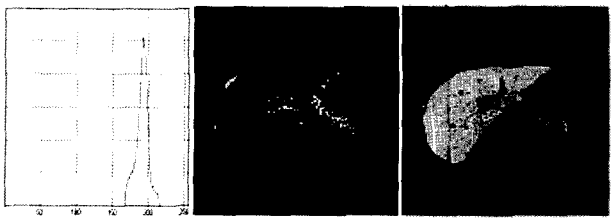

(a) (b) (c)

Fig. 3. Partial histogram thresholding (PHT): (a) the histogram of I_{liver} (b) PHT image I_P, (c) I_{diff}.

4. Binary Morphological (BM) Filtering

BM filtering is processed to remove unnecessary small objects and to smooth the liver boundary. The gray-level image, I_{diff} is transformed to the binary image, B is defined as

$$B=\begin{cases} 1 & \text{if } k_1 \le I_{diff}(m,n) \le k_2 \\ 0 & \text{if } otherwise \end{cases} \quad (6)$$

where k_1 and k_2 are the gray-level range of I_{diff}. BM filtering comes from the combination of biological structure and mathematical set theories [11]. BM filtering is to combine B_{liver} with a structure element, SE through various morphological operations. As the SE is the spatial mask, the 8-connected SE is used in this research. Let $SE_2 \subset Z^2$ SE_2 be a 2 by 2 matrix whose elements are 1 and $SE_3 \subset Z^2$ be a 3 by 3 matrix whose elements are 1.

Basically used BM filtering is dilation and erosion [9, 12]. Let $D^i(B): Z^2 \to Z^2$ be iterative dilation (ID) to extend a region. Let $E^i(B): Z^2 \to Z^2$ be iterative erosion (IE) to reduce a region. ID and IE are defined as

$$D^i(B) = \{\cdots((B \oplus SE) \oplus SE)\cdots) \oplus SE\} \quad (7)$$

$$E^i(B) = \{\cdots((B \ominus SE) \ominus SE)\cdots) \ominus SE\} \quad (8)$$

where B is a binary input image and i is a iteration number. Let, $D^1(B) = D$ $E^1(B) = E$ $D^i(B) = D^i$ and $E^i(B) = E^i$. Let $F(B): Z^2 \to Z^2$ be the 4-connected filling filter.

In order to smooth the boundary, opening and closing filters are used. Let $OP^i(B): Z^2 \to Z^2$ be the iterative opening (IO) filter to smooth thin protrusions. Let $CL^i(B): Z^2 \to Z^2$ be the iterative closing (IC) filter to smooth short gaps. ID and IC are defined as

$$OP^i(B) = \{\cdots((B \circ SE) \circ SE)\cdots) \circ SE\} \quad (9)$$

$$CL^i(B) = \{\cdots((B \cdot SE) \cdot SE)\cdots) \cdot SE\} \quad (10)$$

where B is a binary input image and i is a iteration number. Let $OP^1(B) = OP$, $CL^1(B) = CL$, $OP^i(B) = OP^i$, and $CL^i(B) = CL^i$.

Combination of each filtering has the specific order because the combination order has an influence on the reduction and expansion of the region. Let $CO(B): Z^2 \to Z^2$ be ordered combination function of BM filtering. Used $CO(B)$ in this research is $\{E, F, D, CL^{10}, OP^{10}\}$ with SE_2 and SE_3. Then the binary image obtained by BM filtering is transformed to the gray-level. Let $I_{liver} \subset Z^2$ be a gray-level image. Assuming that B and I have same size, I_{liver} is obtained by pixel by pixel multiplication, $I_{liver} = \{(m,n) \mid B(m,n) \otimes I(m,n)\}$.

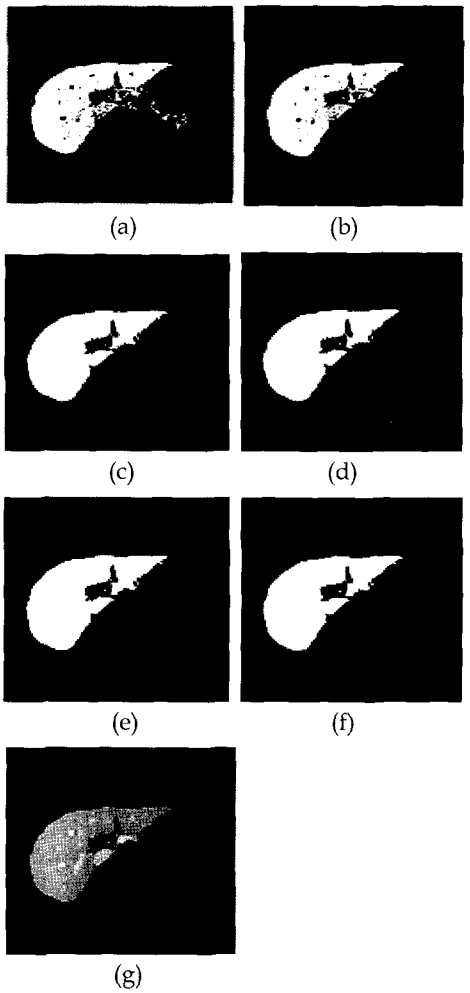

(a) (b) (c) (d) (e) (f) (g)

Fig. 4. BM filtering: (a) binary image, B, (b)B after removing unnecessary objects, (c) filling (d)erosion , (e) dilation, (f) boundary smoothing, (g) gray-level liver, I_{liver}

Fig. 4 shows the example of BM filtering. The binary image, B is shown in Fig. 4(a). The image after removing unnecessary objects is shown in Fig. 4(b). Fig. 4 (c), (d), and (e) show images processed by erosion, filling, and dilation. Also, the liver boundary is smoothed by opening and closing filters shown as Fig. 4 (f). Finally, I_{liver} is created as shown in Fig. 4(g).

EXPERIMENTS AND ANALYSIS

CT images to be used in this research were provided by Chonnam National University Hospital in Kwangju, Korea. The CT scans were obtained by using a LightSpeed Qx/i, which was produced by GE Medical Systems. Scanning was performed with intravenous contrast enhancement. Also, the scanning parameters used a tube current of 230 mAs and 120 kVp, a 30 cm field of view, 5 mm collimation and a table speed of 15 mm/sec (pitch factor, 1:3).

Eight patients were selected for testing the new proposed method to segregate a liver structure. CT images of each patient consisted of 4 slices which were hard to segregate. Also, one radiologist took a part in this research in order to segregate the liver structure by the manual method.

In order to evaluate performance of the proposed algorithm, three different methods were compared such as adaptive multi-modal thresholding with binary morphological filtering (AMT + BM), adaptive multi-modal thresholding, partial histogram thresholding with binary morphological filtering (AMT + PHT + BM) and manual method. The AMT + BM method which was processed by adaptive multi-modal thresholding and binary morphological filtering was called to the automatic segmented method I (ASM I). As the newly proposed method, the AMT + PHT + BM method processed by AMT, PHT, and BM was called to the automatic segmented method II (ASM II). Also, the manual segmented method (MSM) drawn by a radiologist was used for a criterion.

Table 1 shows the normalized average area (NAA) segmented by each method. That is, segmented liver area of each patients were averaged and normalized by the image size. From the results of this comparison, we may know the ASM II including the PHT algorithm has almost same area as the MSM than the ASM I. Also, as the average NAA of ASM I,II, and MSM is 0.2069, 0.1671, and 0.1711 respectively. The NAA difference between ASM II and MSM is very small but ASM I is relatively larger than MSM.

Table 1. Comparison of normalized average area of ASM I, ASM II, and MSM.

	ASM I	ASM II	MSM
Patient 1	0.2125	0.1580	0.1523
Patient 2	0.2285	0.1773	0.1791
Patient 3	0.1893	0.1453	0.1484
Patient 4	0.2457	0.1922	0.2020
Patient 5	0.1344	0.1216	0.1304
Patient 6	0.2836	0.2090	0.2122
Patient 7	0.2066	0.1856	0.1897
Patient 8	0.1545	0.1482	0.1547

As another comparison method, average error rate (AER) is used. The average AER is defined as

$$\text{Average } AER = \frac{|a_{MSR} - a_{ASR}|}{a_{MSR}} \times 100\% \quad (11)$$

where a_{MSR} is the average area of manual segmented rate (MSR) and a_{ASR} is the average area of automatic segmented rate (ASR). The comparison of average AER per each patient based on the MSM between the ASM I and ASM II. The former is 4~40% and the latter is 5~10%. Also, in case of the average of all patients, the former is 24.6238 % and the latter is 6.8339 %.

CONCLUSION

In this paper, we proposed an automatic liver segmentation method using a partial histogram threshold (PHT) algorithm. Histogram transformation such as convolution and scaling was used. Next, adaptive multimodal thresholding (AMT) was performed to find the range of gray-level values of the liver region. We used proposed PHT algorithm. to overcome pixel variation of CE-CT image and remove the pancreas which is contacted with liver. After PHT algorithm, the binary morphological (BM) filtering was processed for removing of unnecessary small objects and smoothing of the boundary.

4 slices of middle liver of CE-CT images from eight patients were selected to evaluate the proposed segmentation method. As the average of normalized average area of the automatic segmentation method II (ASM II) using the PHT and manual segmentation method (MSM) are 0.1671 and 0.1711 respectively. There are very small difference between ASM II and MSM. Also, the average area error rate between the ASM II and MSM is 6.8339 %. From the results of experiments, the proposed method has similar performance as the MSM.

REFERENCES

1. D. M. Parkin, Global cancer statistics in the year 2000, *Lancet Oncology*, Vol. 2, pp. 533-54 2001
2. Hyuk-Sang Lee, *Liver Cancer*, The Korean Society of Gastroenterology, Seoul, Korea 2001
3. Sungkee Lee, *"Extraction of the liver from computed tomography using co-occurrence b matrix"*, J. Biomed. Eng. Res., Vol. 22, No.1, pp. 9-17, 2001
4. K. T. Bae, M. L. Giger, C. T. Chen, and Jr. C.E. Kahn, *"Automatic segmentation of live structure in CT images"*, Med. Phys., Vol. 20, pp. 71-78, 1993
5. L. Gao, D. G. Heath, B. S. Kuszyk, and E. K. Fishman, *"Automatic liver segmentation technique for three-dimensional visualization of CT data"*, Radiology, Vol. 201, pp. 359-364, 1996
6. D. Tsai, *"Automatic segmentation of liver structure in CT images using a neural network"*, IEICE Trans. Fundamentals, Vol. E77-A, No. 11, pp. 1892-1895, 1994
7. S. A. Husain and E. Shigeru, *"Use of neura networks for feature based recognition of liver region on CT images"*, Neural Networks for Sig. Proc.-Proceedings of the IEEE Work., Vol.2, pp.831-840, 2000
8. L. G. Shapiro and G. C. Stockman, *Computer Vision*, Prentice-Hall, Upper Saddle River, NJ, 2001
9. I. Pitas, *"Digital Image Processing Algorithms and Applications"*, Wiley & Sons, Inc. New York, NY, 2000
10. R. J. Schilling and S. L. Harris, *"Applied Numerical Methods for Engineers"*, Brooks/Cole Publishing Com., Pacific Grove, CA, 2000
11. R. C. Gonzalez and R. E. Woods, *"Digital Image Processing"*, 2nd., Prentice-Hall Inc.Upper Saddle River, NJ, 2002
12. B. Jahne, Digital Image Processing, 5th., Springer-Verlag, Berlin Heidelberg, 2002
13. R. A. Schowengerdt, Remote Sensing, 2nd., Academic Press, San Diego, CA, 1997